SESSION D

Thursday, October 22, 1992

1:00 p.m.

Applied Math and Analysis

Papers:

1. Radiation Transport Methods Comparisons Using Computational Benchmarks
   - Bradley Clark (LANL)

2. Fluid Transport and Chemical Kinetics in Chemical Vapor Deposition
   - Bob Kee (SNL)

3. Finite-Difference Methods for Multi-Dimensional Time-Dependent Neutron and Photon Transport Calculations on Lagrangian and Lagrangian-Eulerian Grid
   - Rashit Shagaliev (Arzamas)

4. The Computing Block and Software for an X-Ray Tomography Unit
   - Vyacheslav Krykov, et al (Chelyabinsk)

SESSION D

Applied Math and Analysis

Radiation Transport Methods Comparisons using Computational Benchmarks

Bradley A. Clark, X-6, LANL

Computational Transport theory is an active area of research at all four of the laboratories at this conference. Based upon our experience in other cooperative arenas, exchanges are more productive when there is a strong focus to the meetings, computational benchmark problems can provide that focus. Computational benchmarks are problems that are idealized, in that they do not rely on agreement with a real physical system. The benchmarking is obtained when many different codes and methods are used to analyze a problem. The comparisons between various codes and methods serves to focus discussions at the meetings.

In this paper, we propose a format for such comparisons. It follows the work presented by our colleagues from Arzamaz-16 and Chelyabinsk-70 at the International Symposium on Numerical Transport Theory, sponsored by the Keldysh Institute, and held at Moscow State University in May 1992. At that Symposium, a three dimensional computational benchmark was presented. We would like to add to the collection of problems, which will include simple one-dimensional and two-dimensional problems, as well as more three-dimensional problems. The entire suite of problems would then be analyzed using well-proven techniques and the most modern, and sometimes experimental, finite-difference schemes and acceleration methods. The transport research and collaboration would naturally spring from these discussions.

The International Symposium focused on deterministic methods for solving the transport equation. We would also like to extend these comparisons to stochastic methods. Finally, we would also like to find a forum for discussion of the computational issues associated with solving the transport equation, using deterministic and stochastic methods, on the massively-parallel and distributed computing architectures that will dominate our future computations.

SESSION D

Applied Math and Analysis

FLUID TRANSPORT AND CHEMICAL KINETICS IN CHEMICAL VAPOR DEPOSITION

THE NEED FOR THERMOCHEMICAL AND CHEMICAL-RATE DATA IN CHEMICALLY REACTING FLOW SIMULATION

Robert J. Kee
Computational Mechanics Department
Sandia National Laboratories
Livermore, CA 94551

Computational simulation of chemically reacting fluid flow is playing an increasingly important role in the development, optimization, and control of manufacturing and energy-conversion processes. For example, chemical vapor deposition (CVD) is essential in various stages of semiconductor fabrication. To meet ever-more-stringent electronics-device performance specifications, the performance requirements on the manufacturing process are critical, and often difficult to meet. We are continuing to develop and enhance the computational capabilities that guide the design process. However, while the software tools are able to handle essentially arbitrary process chemistry, the fundamental thermodynamic properties and chemical-kinetic reaction rates are quite often either inadequate or not available.

In semiconductor fabrication applications, CVD may be used to deposit a variety of materials, including polycrystalline or epitaxial silicon, gallium arsenide, silicon nitride, silicon dioxide, silicon carbide, tungsten, copper, and aluminum. Moreover, may of the films require dopants of various materials, like boron or phosphorous. Even for the same desired film material, the processes can use a variety of gas-phase reagents. For many processes that are fully in production today, the chemical kinetics are known only in very empirical terms. The lack of quantitative elementary data significantly impedes our ability to design and optimize new reactors that meet new device requirements. Unfortunately, the amount of data that is required to understand all the processes in production today is enormous, and the cost is correspondingly high.

The application of computational simulation to optimize clean combustion devices, including the incineration of hazardous wastes, is also impeded by the lack of thermochemical and kinetic data, although perhaps less so than for semiconductor device manufacture. Nevertheless, as we become increasingly concerned about high-efficiency combustion (lowering CO_2 emissions), reduction of NO_x and SO_x, and compliance with new legislation (e.g. regulation of air-toxics), the task of designing and controlling new combustion devices will rely increasingly on the ability to simulate the processes and consider tradeoffs.

We suggest that employing chemical-physics institutes in the former Soviet Union may provide a cost-effective route to measuring the thermochemical and kinetic data that is required to derive the full benefit of our computational-simulation capabilities. We presume that hundreds of Eastern-block scientists may be available to undertake measurement of the required data, and at a fraction of the cost that would be required in the West.

SESSION D

Applied Math and Analysis

Finite-difference methods for multi-dimensional time-dependent neutron and photon transport calculations on Lagrangian and Lagrangian-Eulerian Grid

Alekseyev A.V., Yevdokimov V.V., Moskvin A.N.,
Pletenyova N.P., Fedotova L.P., Shagaliyev R.M., Shumilin V.A.

The All-Union Institute of Experimental Physics.

The report presents Saturn finite - difference methods for the multi-dimensional time - dependent transport equation .

Approximation issues are discussed for a 2-D transport equation solved on various nonorthogonal spatial grids.
We focus on the accuracy desired for difference schemes on highly distorted grids.

Iteration algorithms are proposed for numerical solution of high-dimension difference transport equations. The efficiency of generated schemes and numerical methods is illustrated by test neutron and thermal radiation transfer calculations.

The methods proposed generalize to the numerieal solution of a 3-D group transport equation.

Parallelization algorithms are discussed for numerical solunion of a multi-dimensional transport equation.

Finite-difference methods for multi-dimensional time-dependent neutron and photon transport calculations on Lagrangian and Lagrangian-Eulerian Grid

Alekseyev A.V., Yevdokimov V.V., Moskvin A.N.,
Pletenyova N.P., Fedotova L.P., Shagaliyev R.M., Shumilin V.A.

The All-Union Institute of Experimental Physics.

Computer simulation of time-dependent neutron and photon transport processes and particle/medium interaction is an important part of many applications.

Lagrangian or Lagrangian/Eulerian medium motion should be often accounted to perform time-dependent transport calculations. In those cases, the transport equation must be approximated using imposed (generally) nonorthogonal spatial grids that vary with time and may experience substantial deformations changes during calculations.

For the class of problems under consideration, the most important requirement is that numerical methods for the transport equation should provide the desired accuracy and cost-efficiency on a broad class of nonorthogonal spatial grids.

This report presents finite-difference methods for time-dependent spectral spatial 2-D and 3-D transport calculations implemented within code package SATURN . Note that SATURN allows to calculate transfer processes using both transport and diffusion multigroup approximations. This report restricts to the issues involved in transport approximation.

For this approximation, the boundary-value problem formulation includes the following types of multigroup systems /1,2/.

I. Neutron transport and multiplication

$$\frac{1}{V_i}\frac{\partial N_i}{\partial t} + LN_i + \alpha_i N_i = F_i, \qquad i=1,2,\ldots,i_1 \qquad (I)$$

where in the 2-D case

$$LN_i \equiv \frac{1}{r}\frac{\partial}{\partial r}(r\cdot\cos\Psi\cdot\sqrt{1-\mu^2}\cdot N_i)+\frac{\partial}{\partial z}(\mu\cdot N_i)-\frac{\partial}{\partial\Psi}\left(\frac{1}{r}\cdot\sin\Psi\cdot\sqrt{1-\mu^2}\cdot N_i\right),$$

$$F_i \equiv \frac{1}{2\pi}\sum_{j=1}^{i-1}\beta_{ij}\,n_j^{(0)}+\frac{1}{2\pi}\cdot Q_i, \qquad (2)$$

$$n_i^{(0)}=\int_{-1}^{1}\int_{0}^{\pi} N_i\,\partial\Psi\,\partial\mu,$$

and in the 3-D case

$$LN_i \equiv \frac{1}{r}\frac{\partial}{\partial r}(r\cdot\cos\Psi\cdot\sqrt{1-\mu^2}\cdot N_i)+\frac{\partial}{\partial z}(\mu\cdot N_i)-\frac{\partial}{\partial\Psi}\left(\frac{1}{r}\cdot\sin\Psi\cdot\sqrt{1-\mu^2}\cdot N_i\right)+$$

$$\frac{1}{r}\frac{\partial}{\partial\varphi}(r\cdot\sin\Psi\cdot\sqrt{1-\mu^2}\cdot N_i), \qquad (3)$$

$$F_i \equiv \frac{1}{4\pi}\sum_{I=1}^{i-1}\beta_{ij}\,n_j^{(0)}+\frac{1}{4\pi}\cdot Q_i,$$

$$n_i^{(0)}=\int_{-1}^{1}\int_{0}^{2\pi} N_i\,\partial\Psi\,\partial\mu$$

The systems (1),(2) and (1),(3) represent the conventional formulation. Note, that SATURN allows more complex neutron and nuclear processes to be calculated, particularly anisotropic scattering, neutron retarding and isotope transition kinetics can be accounted.

II. Thermal radiation energy transport and radiation/material interaction(2-D formulation):

$$\frac{1}{c}\cdot\frac{\partial F_i}{\partial t}+LF_i+\varkappa_{ni}\cdot\varepsilon_{ip}=F_{ip}, \qquad (4)$$

$$F_{ip}\equiv\frac{1}{2\pi}\left(\varkappa_{ni}\cdot\varepsilon_{ip}+\varkappa_{si}\sum_{j=1}^{i}a_{ij}\varepsilon_j^{(0)}\right);$$

$$\rho\cdot\frac{\partial E}{\partial t}=\sum_{i=1}^{i-1}\varkappa_{ni}\varepsilon_i^{(0)}\Delta\omega_i-\sum_{i=1}^{i-1}\varkappa_{ni}\varepsilon_{ip}\Delta\omega_i- \qquad (5)$$

$$\sum_{i=1}^{i-1}\varkappa_{si}\sum_{j=1}^{i-1}a_{ij}F_j\,\Delta\omega_i$$

Here

ε_{ip} - Planck function,

(a_{ij}) - j-to-i photon transition matrix under Compton scattering.

SATURN makes it possible to model Compton scattering using both elastic and nonelastic approximations. In the first case the matrix $(a_{i,j})$ is unity while in the second case it is completely filled and depends on temperature.

The electron temperature can be accounted.

In the 2-D case the finite-difference approximation of the transport equation uses two classes of spatial grids.

First, these are represented by regular (matrix) nonorthodonal grids consisting of quadrangles. Note, that the major part of 2-D calculations uses principally this class of grids.

Second, irregular grids consisting of convex polygons are used. For many years irregular Lagrangian and Lagrangian/Eulerian gasdynamic methods are successfully applied to the most complex 2-D calculations characterized by severe local deformations when performing the computations /3/. The interest to developing numerical methods to solve the transport equation on such grids arised from that these computations should be performed together.

We use an extended-template scheme to approximate the time-dependent transport equation on nonorthogonal grids /4/. Note, that this scheme is of DSn-type /5/. The scheme under consideration is remarkable for that function values are introduced at the grid nodes (cell vertices) along with average values of the function to be found on edges and in cells usually used in DSn schemes. Using this extended template allows to derive additional relations by representing the in-cell solution as linear functions along some straight lines irrespectively of how many sides of quadrangular cells are visible. As the results of numerical studies show, the extended template scheme has the convergence accuracy order close to the second one even on highly distorted grids /4/.

This scheme generalizes to polygon mesh in a natural manner. The new problem which had to be solved in this case is to ensure the nondegeneracy for the matrix of mesh equations corresponding to a single spatial cell.

In addition to the finite-difference approximation, another question is of high importance when developing finite-difference methods for transport problems: whether it is possible or not to obtain a cost-efficient numerical solution for a system of multigroup difference equations on timesteps.

This question becomes crucial for thermal radiation transfer calculations where the optical properties of systems calculated vary in a broad range and the multiplication coefficient is close to unity in many cases.

A special attention is now paid to the development of efficient numerical methods for systems of difference transport equations (see, for example,/6/-/11/).

Most of the methods used are known to rely upon the combination of the iterations over the RHS (collision integral) and algorithms for acceleration of this iterative process. The most complex problem arising from this approach and most severely pronounced in optically dense calculations with the multiplication coefficient close to unity is how to provide the consistence between the transport operator and the operator from the "accelerating"equation in a difference form (/6/-/9/, /11/).

SATURN implements several algorithms to solve numerically the system of difference group transport equations. One of them will be considered in more details and further referred to as KM method for the sake of brevity /12/.This is a two- step method of predictor-corrector type with re-iterations over the time variable of the following form:

$$\frac{1}{V_i}\cdot\frac{N_i^{s+1/2} - N_i^{n}}{\Delta t} + LN_i^{s+1/2} + \alpha_i N_i^{s+1/2} = \frac{1}{2\pi}\sum_{j=1}^{i-1}\beta_{ij}\,\bar{n}_j^{(s)} + \frac{1}{2\pi}\,Q_i, \qquad (6)$$

$$\frac{1}{V_i}\cdot\frac{N_i^{s+1} - N_i^{n}}{\Delta t} + LN_i^{s+1} + \alpha_i N_i^{s+1} - \sum_{j=1}^{i-1}\beta_{ij}\,N_j^{s+1} = \qquad (7)$$

$$= \frac{1}{2\pi}\sum_{j=1}^{i-1}\beta_{ij}\,\bar{n}_j^{(s+1/2)} - \sum_{j=1}^{i}\beta_{ij}N_j^{s+1/2} + \frac{1}{2\pi}\,Q_i, \qquad i=1,2,\ldots i_1$$

As can be seen from the above form, specific features of this algorithm are as follows: explicit computation of the collision integral on both KM halfsteps, actual stability of the algorithm for computations with a limited number of iterations,numerical solution conservatism, cost-efficient solution of the system of mesh equations with the known RHS, consistent finite-difference approximation of equations corresponding to separate stages.

These features provide a sufficiently high efficiency of the method particularly for thermal radiation transport

Computational results from /12/ are given below for three problems solved with KM method. Note that the first two problems are in slab geometry .

Computational results for these problems solved using different timesteps are given in Table I.

Table I.

Computational results for optically thin case I and optically thick case 2

*	Δt	**	***		ε = 0.1		ε = 0.01	
			$s_\varepsilon^{(0)}$	N_i	$s_\varepsilon^{(0)}$	N_i	$s_\varepsilon^{(0)}$	N_i
1	0.0625	320	23.8600	1	23.8600	1	23.8602	1.1
	0.125	160	23.8760	1	23.8767	1.01	23.8772	1.41
	0.25	80	23.9416	1	23.9411	1.04	23.9385	1.88
	0.5	40	24.2234	1	24.1583	1.13	24.2060	2
	1	20	25.6070	1	25.1163	1.5	24.3016	2
2	0.075	480	8546.26	1	8545.30	1.75	8547.41	3.48
	0.15	240	8544.18	1	8547.59	4.49	8547.42	7.78
	0.3	120	8540.14	1	8547.01	5.48	8547.44	12.12
	0.6	60	8539.32	1	8540.95	4.77	8546.50	12.4
	1.2	30	8554.51	1	8536.34	8	8545.62	20.87
	2.4	15	8526.48	1	8534.18	12.27	8546.50	39.73

* Case
** Number of time steps
*** Without re- iterations

The next problem is the well known Fleck problem /13/. This was solved using the 28 group approximation in two models which differed in timestep size.Furthermore, the calculations were also performed for 2-D case. Figures 1 and 2 show calculated temperature wave profiles for several times.

For more details on problem formulation and calculational results refer to/12/.

Finally, it should be noted that the KM method converts to the well known iterative deviation estimate method /14/ in a stationary one-velocity case. Therefore, the KM method can be also considered a generalization to nonstationary and multigroup case for the above mentioned method.

Moreover, SATURN implements the algorithms for acceleration of

the iterative process within a single energy group in addition to the KM method oriented to combined numerical solution for the system of group difference equations accounting intergroup particle transitions. These algorithms are conceptually close to techniques reported in /8,14/.We shall not consider them further because of limited report size.

Currently, individual region computations are used in computational physics where the initial geometry is split into separate subregions (mathematical or computational regions); the equations are approximated on separate spatial grids inside subregions, subregion interinfuence is accounted by exchanging the inner boundary conditions.

SATURN uses an iterative version of regional computations for numerical 2-D time-dependent transport calculations. Directional flow function is used as inner boundary conditions. Since the iterative process over inner boundary conditions converges rather slowly for a number of important applications solved numerically, a special acceleratin algorithm was developed for the convergence of the iterative process over inner boungary conditions. Note,that this algorithm relies upon the combined mesh solution on the inner boundaries obtained on two KM half-steps.

The desired accuracy of the numerical simulation for some classes of transport problems is only possible in 3-D case. We shall introduce the following classes of spatial grids for finite-difference approximation of the 3-D transport eguation (1),(3) written in cylinder coordinates.

Split the original body into many sectors (F-sectors) by planes leaves passing through the rotational axis Z. Construct nonorthogonal regular grids consisting of convex quadrangles and containing the same number of rows and columns indicated leaves. Then one obtains the desired hexahedron grid for 3-D calculations by connecting corresponding vertices of respective quadrangles.

Approximate the transport eguation on the obtained grid using a difference scheme which is an extended template scheme generalized to the 3-D case /12/There exist six versions of approximation for the transport equation in 3-D case depending on the number of visible cell faces. Note, that five of them use additional relations based on the in-cell solution represented as linear functions along some straight lines.This gives the second-order

accuracy (or close to it) for the approximation of the transport equation. The latter variant corresponds only to one visible side of a cell and is based on the in cell representation as a constant which generally gives only first order approximation of the transport eguation.In this view it should be noted that the latter approximation was not used for orthogonal grids. As the compulational experience shows, the version 6 is rarely applied to the transport eguation (though if is) for the general nonorthogonal grid and is not crucial for the solution accuracy.

The system of equations arising on a single timestep in a 3-D case is very large (about 10^7equations). When the transport equation right- hand is specified, this system is solved using a special cost-efficient running computation algorithm based on the combination of the running algorithm /16/ and intra-block iterations.

Then we use the inner iterations to solve the system of difference equations in a general case, when the right-hand side is unknown.

The iteration convergence speed is inceased by using special accelerating algorithms which were obtained by generalizing some algorithms used in the 2-D case.

SATURN that implements the above numerical methods runs on the Elbrus-2 multiprocessor. We use several parallelization algorithms, to reduce the time of 2-D and 3-D time-dependnt transport calculations.

For 2-D calculations, the parallelization is done over energy groups and computational regions. For 3-D computations, a deeper pipelined parallelization is used which allows several directions, F-sectors and energy groups to be computed in parallel.

Table 2 contains the computational results for a series of 3-D test calculations performed to estimate the parallelization algorithm.

Table 2.

# of processors	1	2	3	4	5	6	7	8	9	10
Gain (single tasking)	1	1.97	2.93	3.88	4.89	5.48	6.10	6.92	7.65	8.29
Gain (Multitasking)	1	2.1	3.2	4.2	4.8	5.3	5.9	6.1	6.5	6.6

As the results show, the parallelization algorithm allows to reduce substantially the computation time for 3-D transport calculations. Note, that the overhead is relatively small.

Finally, we should point out that the numerical methods and algorithms discussed here and implemented in SATURN are successfully used for broad classes of mulitidimensional time-dependenf neutron and photon transport calculations and particle /medium interaction for several years. The calculations include gasdynamic medium motion and many other processes.

References

1. Davision W., Neutron transport theory. (in Russian), Moscow, Gosatomizdat,1960.
2. Zeldovitch Ya.B., Reiser Yu.P., Shock wave and high-temperature hydrodynamic phenomena physics, Moscow, Nauka, 1966.
3. Sofronov I.D., Rasskazova V.V., Nesterenko L.V., The use of Nonregular Nets for solving two-dimensional Nonstationary problems in gas dynamics, Advances in Science and Technology in USSR, M., Mir, 1987.
4. Pleteniova N.P., Shagaliev R.M., Approximation of 2-D transport equation on quadrangular and polygon spatial grids with extended template difference scheme. VANT, Ser.: Mat. Modelir. Fiz. Proc., 1989, no.3, p.34-41.
5. Carlson B.G., The numerical theory of neutron transport methods in computational physics. Acad. Press. 1963, vol.1, no.9, p.408-425.
6. Troshchijov V.E., The solution of transport and quasidiffusion equations using consistent difference schemes. Numerical methods for calculations in computational physics, M., Nauka, 1966, p.177-185.
7. Reed W.H. Effectiveness of acceleration techniques for Iterative Methods in Transport Theory. Nucl. Sci and Eng., 45, 245-254 (1971).
8. Alcouffe R.E.
   a) Diffusion Synthetic Acceleration Methods for the Diamond-Differenced Discrete-Ordinates Equations. Nucl. Sci. and Eng. 64, 344-355 (1977),
   b) Diffusion-Accelerated Sn-Transport Method for Radiation

Transport on a General Quadrilateral Mesh. Nucl. Sci. and Eng. 105, 191-197 (1990).
9. Yudintsev V.F., Convergence of iteration speedup correction methods for transport equations in difference form. Numerical methods in mechanics of continuum 1981, vol.12, no.5, p.148-165.
10. Troshchijov V.E., Shumilin V.A., Difference scheme for solving the 2-D transport equation on irregular quadrangular grids., Journal of Comput.mathematics and physics, 1986, vol.26, no.2, p.230-241.
11. Bass L.P., Voloshchenko A.M., Germogenova T.A., The discrete ordinate method in radiation transport problems, M., IPM, 1986.
12. Fedotova L.P., Shagaliev R.M., Finite-difference KM-method for computer transport processes using multigroup transport approximation, Computer simulation, 1991, vol.3, no.6, p.29-41.
13. Fleck J.A., Cummings J.D. An implicit Monte-Carlo scheme for calculating time and frequency dependent nonlinear radiation transport. J.of Comput.Phys., 1971, Vol.8, p.313-342.
14. Morozov V.N., Solving kinetic equations with Sn method, Theory and methods for reactor calculations, M., Gosatomizdat, 1962, p.91-117.
15. Zaguskin V.L., Kondrashov V.E., Solving heat conduction and gas dynamics equation by separate regions, Proc. of Ac. of Sci., 1965, vol.163, No 5,p.1107-1109.
16. Troshchijov V.E., Classes of meshes allowing the approximation of the 2-D transport operator with triangular difference operator, J. of Comput. Math. and Phys., 1976, vol. 6, no.3., p.793-797.

Fig. 1 Fleck J.A., Cummigs J.D. problem.

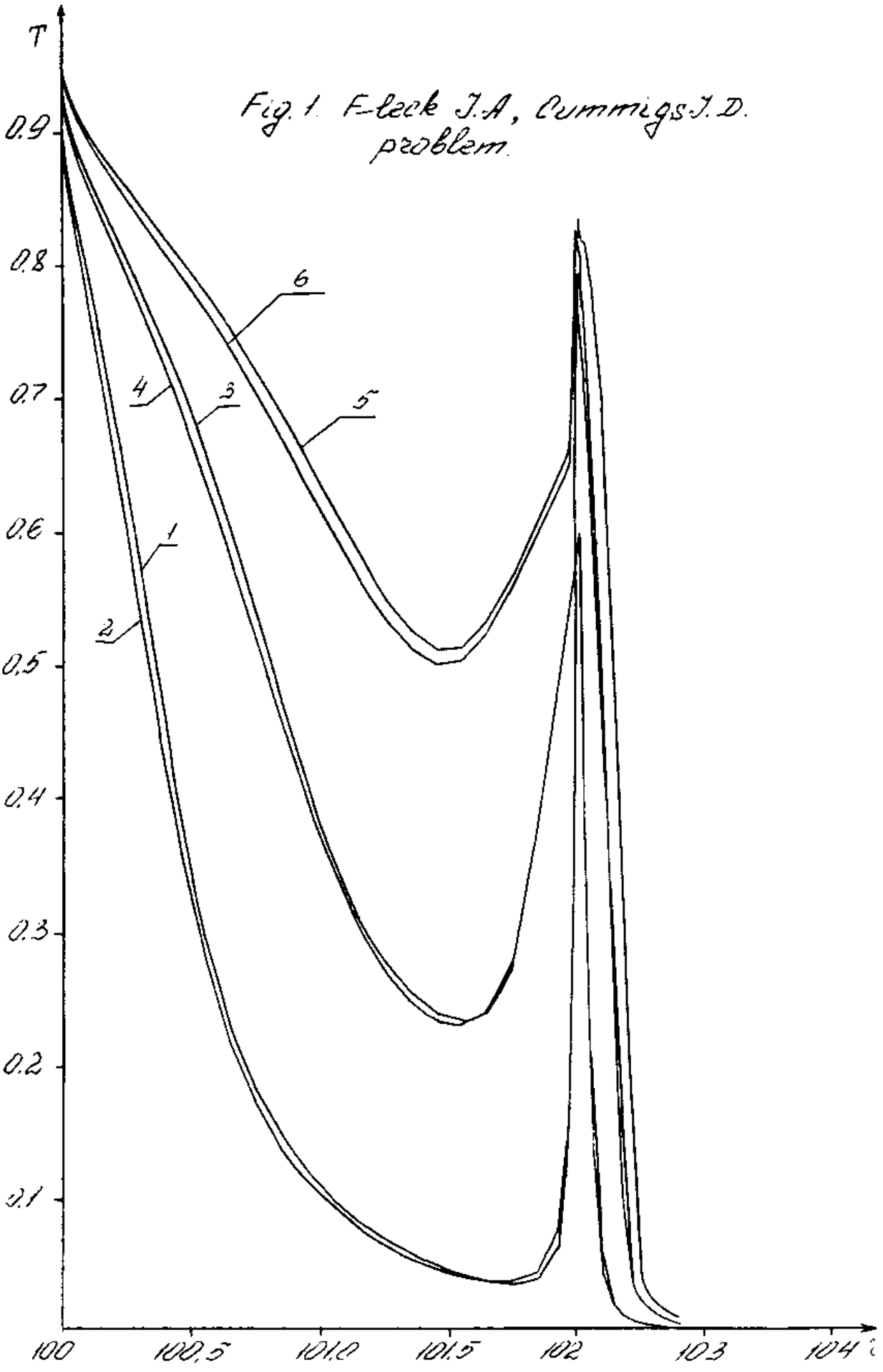

Temperature profiles for several times ($c \cdot \Delta t = 0.3, 6.9$)

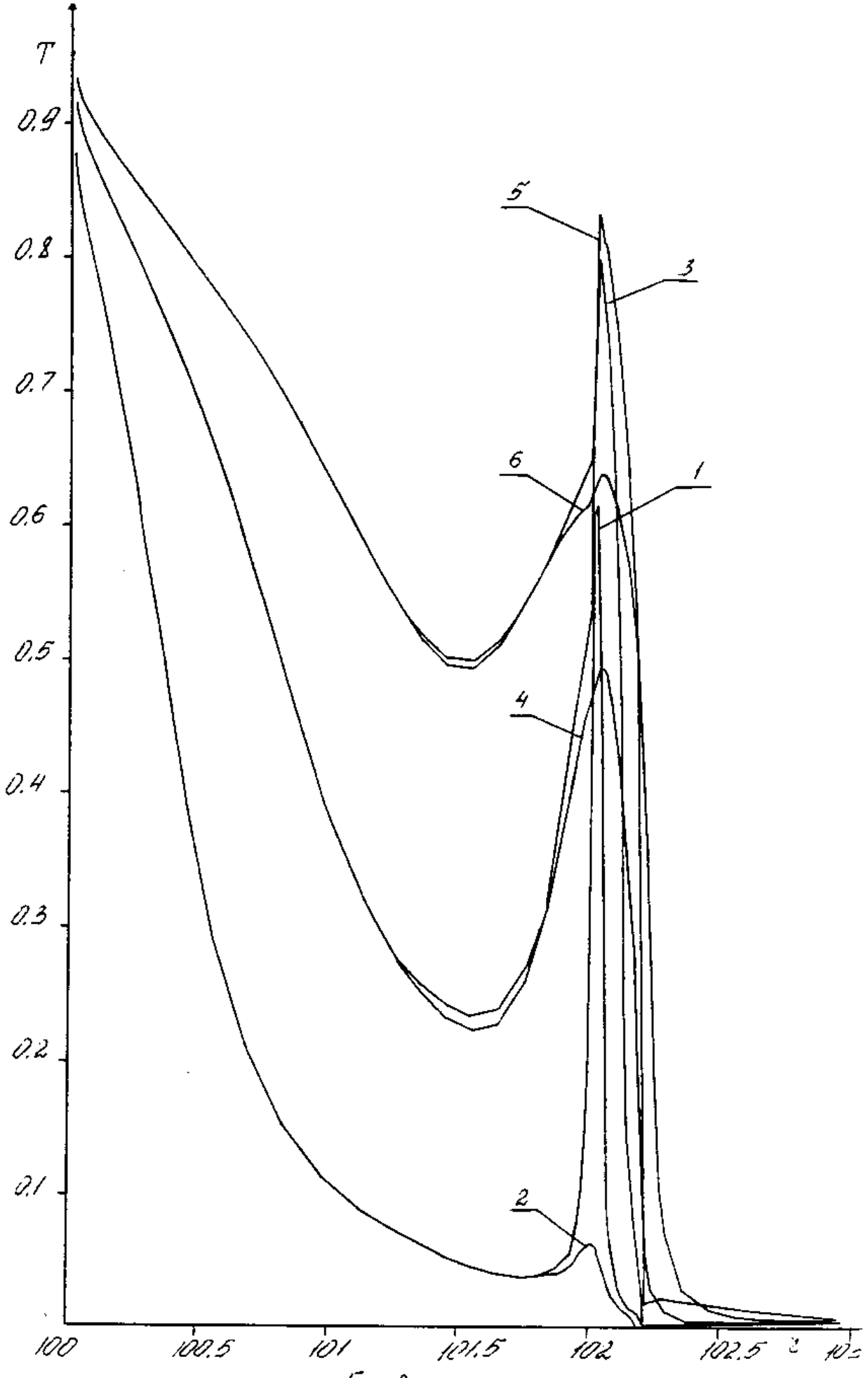

Fig.2.

Temperature profiles for several

SESSION D

Applied Math and Analysis

The Computing Block and Software for an X-Ray Tomography Unit
Vyacheslav Krykov, et al. (Chelyabinsk)

D-4

THE COMPUTING BLOCK AND SOFTWARE FOR AN X-RAY TOMOGRAPHY UNIT

Kryukov V.M., Konotop Yu.I., Romanova E.M., Fedorov V.V.

Introduction

The development of a computer-aided X-ray tomography unit (CXTU), for medical applications, entails, among other things, the solving of problems in mathematical modeling of the optical path of the X-rays, the design of a computing block, and the generation of appropriate software. The mathematics department of the Russian National Nuclear Center of the All-Union Scientific Research Institute of Engineering Physics has considerable experience in numerical modeling of the transport of various types of radiation (neutrons, photons, electrons, charged particles) with allowances for their mutual transformations. This knowledge is now being applied to problems in medical physics, such as radiation therapy and diagnostics. A separate presentation could be devoted to a detailed discussion of those topics.

The present discussion concerns the development of the computing block and the associated software for a tomography unit having the following specifications:

-Density resolution for details above 3.5mm and at density levels corresponding to those of water: not less than 0.5% with a 10% contrast level for details of 1.0mm.

-Field of view in the scanning plane: 480mm minimum.

-Scan time for one section: 4-12 sec.

-Maximum image reconstruction time after completion of scan: 10 sec.

-Array size of the reconstructed image: 512 x 512.

-Minimum number of grey-levels: 64.

The Computing Block

The computing block (CB) is at the center of the CXTU (Fig.1), with all control lines for the various subsystems converging on it. In addition to providing an interface between the operator and the machine, the CB loads all the control parameters for a given examination procedure into the automatic control unit (ACU), receives data on the absorption of X-rays by the patient's tissues from the data collection unit (DCU), performs the computation-intensive image reconstruction and, finally, executes the image processing and data extraction routines needed by the medical personnel.

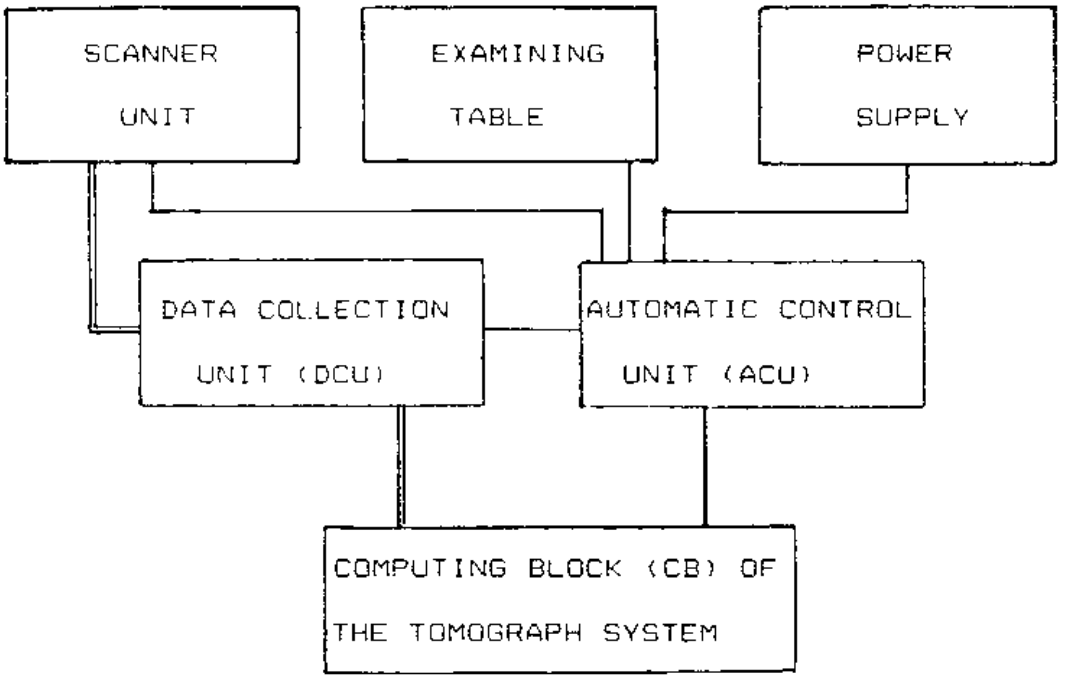

Fig. 1. Position of the computing block in the tomography system

The computing block of the CXTU is unique by virtue of a number of functional blocks that are now being designed for it (Fig. 2). A personal computer is used as the control unit for the CB. The bulk of the computations is handled by a special processor. The operator interface is effected through a keyboard, a mouse, and a special control console. A video display and a hard-copy output are provided.

Image data from the DCU are passed into the special processor where the basic computational tasks of image restoration are performed: the preliminary processing (PP) of raw data, the projection filtering (PF), and the reverse projection (RP).

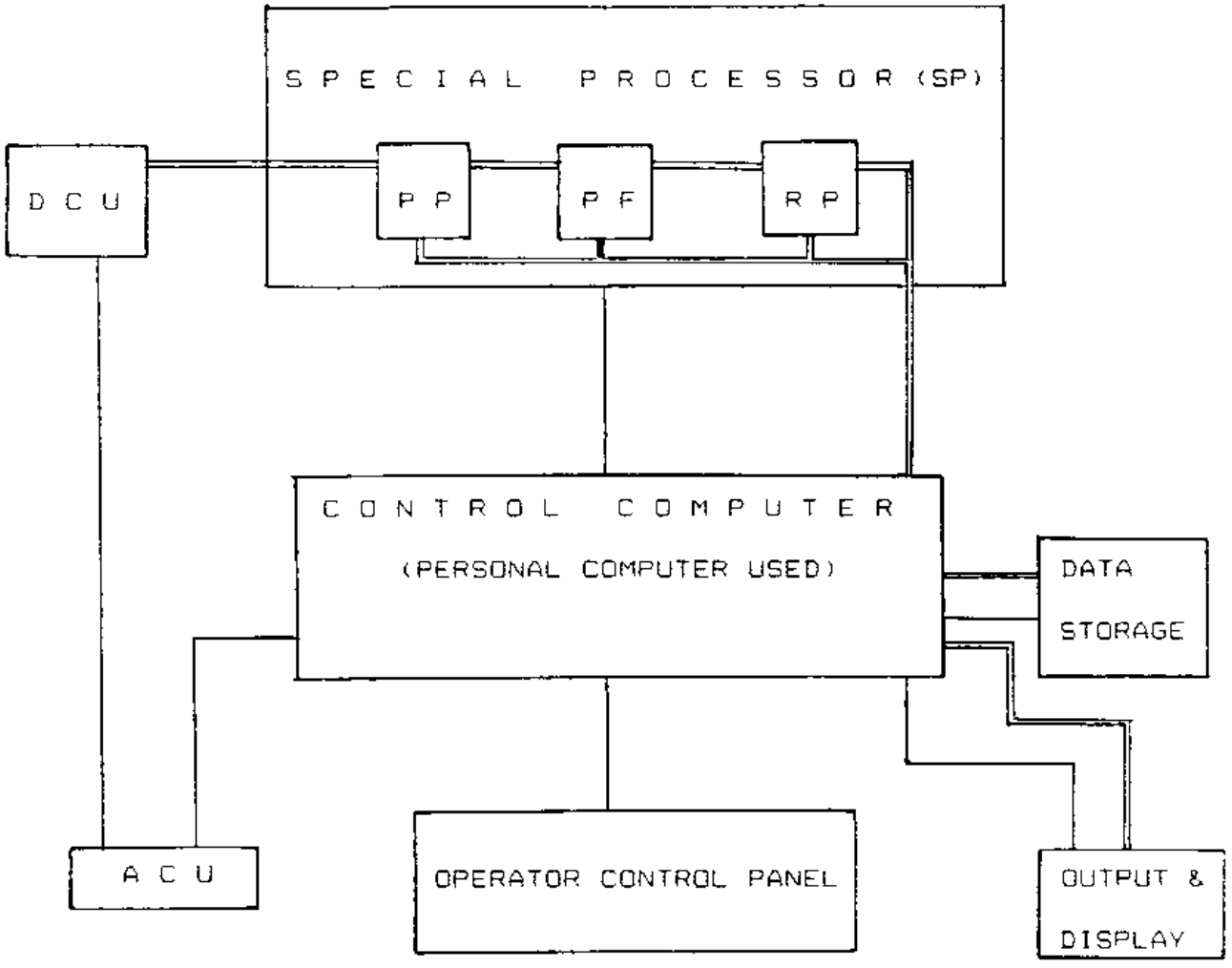

Fig.2. Functional block diagram of the CB

The matrix of the reconstructed image is filtered in the special processor in accordance with a given algorithm and passed on to the control computer. Data from the DCU and the reconstructed images are recorded on magnetic disks or tape. Data compression techniques may be used in the process.

The PP block performs the verification and error correction of sensor data, subtracts the "substitution value", converts the results obtained into a logarithmic form, corrects for radiation dispersion, normalizes the channels to compensate for their nonuniformity, receives the outputs from the support sensors, and corrects for the polychromaticity of the X-ray emission. All these functions are not computation-intensive and are executed in the PP block at the rate at which the projections are introduced.

The projection filtering utilizes various functions (nuclei): those of Shepp-Logan, Lakshminarayan-Ramachandran, Reece, Tuci and others. The PF block processes the projections at the rate at which they arrive from the PP block.

Particular complications in the design of the CB arise from the special-processor block, which implements the reverse-projection algorithm and which must process the data at a high speed. The reverse-projection algorithm can be readily made to work in a parallel fashion, which simplifies the task of designing a high-speed RP block, and may be accomplished by various means, for example:

1. The image matrix is broken up into quadrants or strips. Each portion of the matrix is reconstructed by a separate processing block (PB). Complete filtered projections are fed to the input of each PB, and each PB outputs its portion of the reconstructed image (Fig. 3).

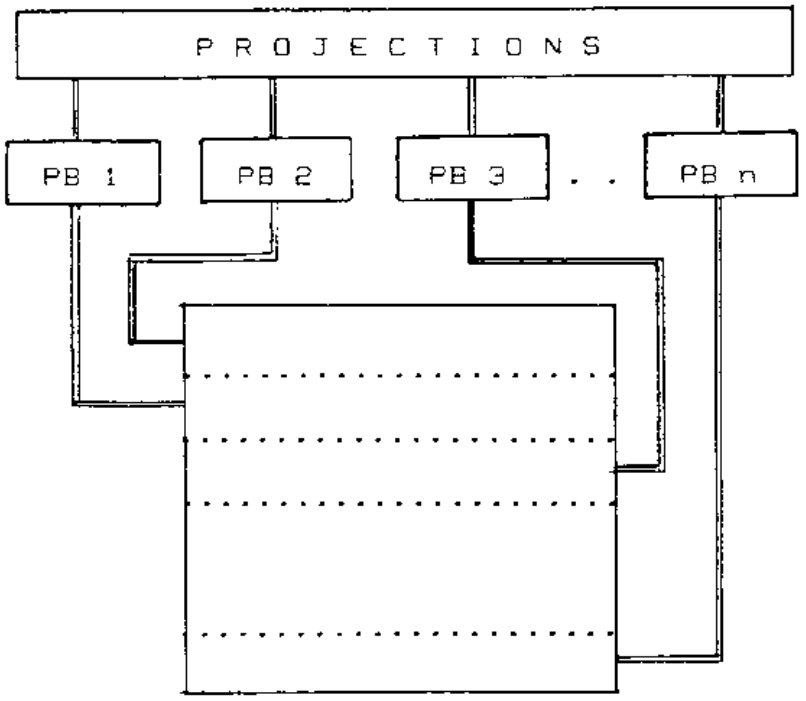

Fig.3 Parallel operation of the RP block (version 1).

2. The RP block contains several PBs each of which computes a value to be added to an element of the matrix that is being reconstructed on the basis of a given filtered projection. Connected in series, the PBs constitute a conveyor in which the summary addition to the matrix elements is accumulated for all the projections that are being processed simultaneously (Fig. 4).

In each version, the number of the PBs selected is based on their efficacy and on the time required for the generation of a tomogram after the scanning has been completed. If the cumulative

speed of processing of the projections in the RP block is lower than the rate at which the projections arrive from the PF block, a RAM buffer is used to compensate for the difference in speed.

In order to test the separate blocks of the special processor and to evaluate the repetitive image reconstruction, a feature is being implemented which will permit loading the initial data into the special processor from the control computer (CC), and unloading the results into the CC, after processing the data by the PP and PF blocks.

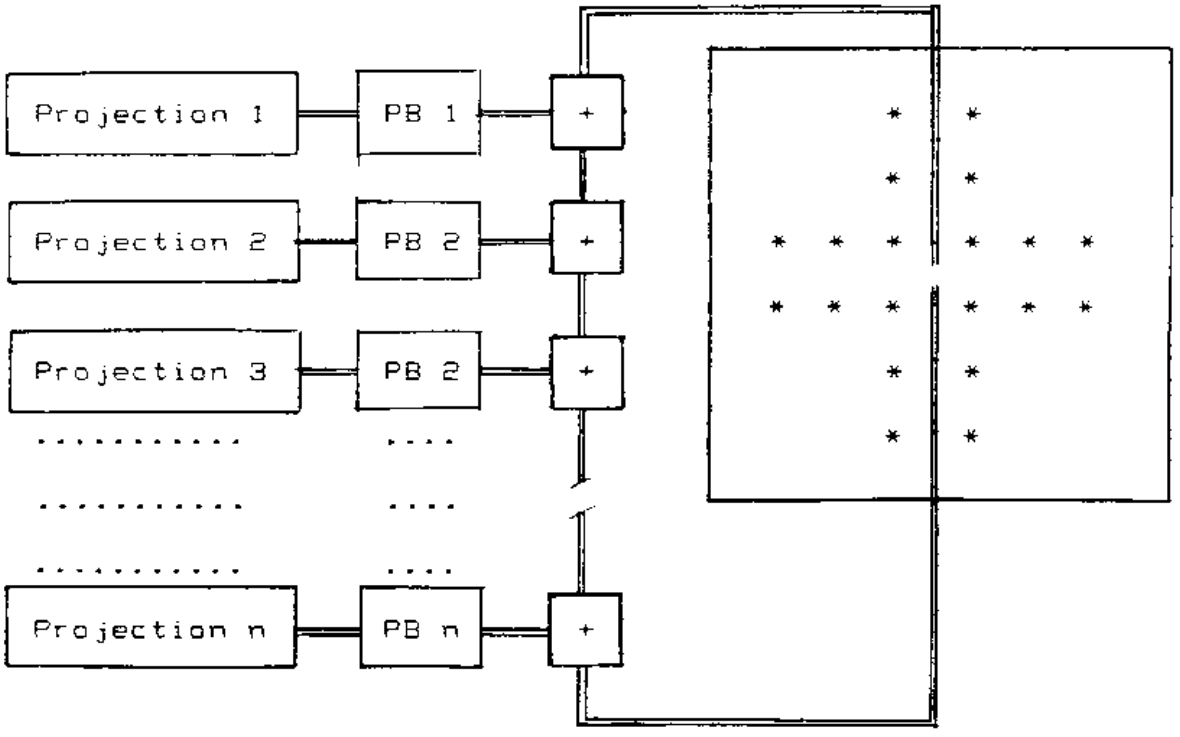

Fig.4. Parallel operation of the RP block (version 2).

The special processor may be implemented as a hardware algorithm for image reconstruction or as a universal multi-processing computational accelerator.

Software

The tomograph software (TS) must offer the operator maximal convenience in both the examination of the patient and in processing of the resultant data.

To this end, subsystems are being developed that will provide the following features:

-A library of readily selectable, standard routines for the examination of the head, neck, chest, abdomen, and the extremities.

- A means of registering a new patient and accessing a catalog of patients who had been examined in the past.

-A means of "bench marking" the patient with reference to the examining table and generating tomographic sections by using topograms to aim at targets.

-A means of visualizing and analyzing of tomograms.

-Repetitive image reconstruction in areas of interest based on prior projection data.

-Generation of sagittal and coronary sections.

-Construction of three-dimensional images based on multiple sections.

-Preparation of documentation with hard-copy capability.

-Operational aids for the operator such as a menu and a brief listing of capabilities available at any given point in the examination process.

The software provided for the visualization and analysis of the tomograms enables the operator to select the most convenient graphical technique, e.g.:

-A dot cursor for designating a point on the tomogram.

-A line cursor to indicate a vertical or horizontal line on the tomogram.

-A "frame" in the shape of a rectangle, circle, ellipse or any arbitrary enclosed curve to define the area of interest.

-Segments of angles and grids for geometric measurements.

-An arrow to mark and select various areas on the monitor screen.

The following capabilities are available in the tomogram analysis mode:

-Determination of density at a given point.

-Availability of statistical data for the area of interest (average density, minimum and maximum density values, dispersion, and standard deviation).

-Generation of a density distribution plot along a line cursor.

-Generation of a density distribution histogram for a designated area of interest.

-Measurement of distances and angles constructed by segments.

-Measurement of the area of interest.

-Use of various filters for image processing (smoothing, contrast-enhancement).

-Magnification of a selected portion of the image by 2X to 10X.

-Rotation of the image through 90, 180, and 270 degrees.

-Symmetrical transformation with respect to the vertical or horizontal axes.

-Generation of negative images.

-Subtraction and addition of images.

-Adjusting of boundaries of the visible density interval.

-Adjusting of the density transformation function in grey levels when in tomogram visualization mode.

When in documentation mode, the TS will have the capability to superimpose comments onto the image, assemble anywhere from two to nine images into one document, and provide a hard-copy output.

Currently in design are subroutines which will provide the following capabilities:

-Adjustment of the individual subsystems of the tomograph.

-Calibration of the data collection system.

-Adjustment of sensors.

-Testing.

All the subsystems are controlled by one unit. To this end, an appropriate programming shell is being developed.

Status of the project, current problems.

The computing block and the software portion of the tomograph project are in the development stage. The overall architecture of the computing block has been defined. The communication hardware for linking the tomograph subsystems is being built for the laboratory prototype unit. The special processor is being designed and built in two versions: as a universal processor and as a processor in which the image reconstruction algorithm is implemented in hardware. The development of software for the visualization and image analysis functions is 50% complete. The software for the control of the tomograph subsystems is in design.

The problem is the absence of high-speed LSI chips suitable for the creation of a compact and reliable special processor.

THE COMPUTING BLOCK AND SOFTWARE FOR AN X-RAY TOMOGRAPHY UNIT

Kryukov V.M., Konotop Yu.I., Romanova E.M., Fedorov V.V.

Introduction

The development of a computer-aided X-ray tomography unit (CXTU), for medical applications, entails, among other things, the solving of problems in mathematical modeling of the optical path of the X-rays, the design of a computing block, and the generation of appropriate software. The mathematics department of the Russian National Nuclear Center of the All-Union Scientific Research Institute of Engineering Physics has considerable experience in numerical modeling of the transport of various types of radiation (neutrons, photons, electrons, charged particles) with allowances for their mutual transformations. This knowledge is now being applied to problems in medical physics, such as radiation therapy and diagnostics. A separate presentation could be devoted to a detailed discussion of those topics.

The present discussion concerns the development of the computing block and the associated software for a tomography unit having the following specifications:

-Density resolution for details above 3.5mm and at density levels corresponding to those of water: not less than 0.5% with a 10% contrast level for details of 1.0mm.

-Field of view in the scanning plane: 480mm minimum.

-Scan time for one section: 4-12 sec.

-Maximum image reconstruction time after completion of scan: 10 sec.

-Array size of the reconstructed image: 512 x 512.

-Minimum number of grey-levels: 64.

The Computing Block

The computing block (CB) is at the center of the CXTU (Fig.1), with all control lines for the various subsystems converging on it. In addition to providing an interface between the operator and the machine, the CB loads all the control parameters for a given examination procedure into the automatic control unit (ACU), receives data on the absorption of X-rays by the patient's tissues from the data collection unit (DCU), performs the computation-intensive image reconstruction and, finally, executes the image processing and data extraction routines needed by the medical personnel.

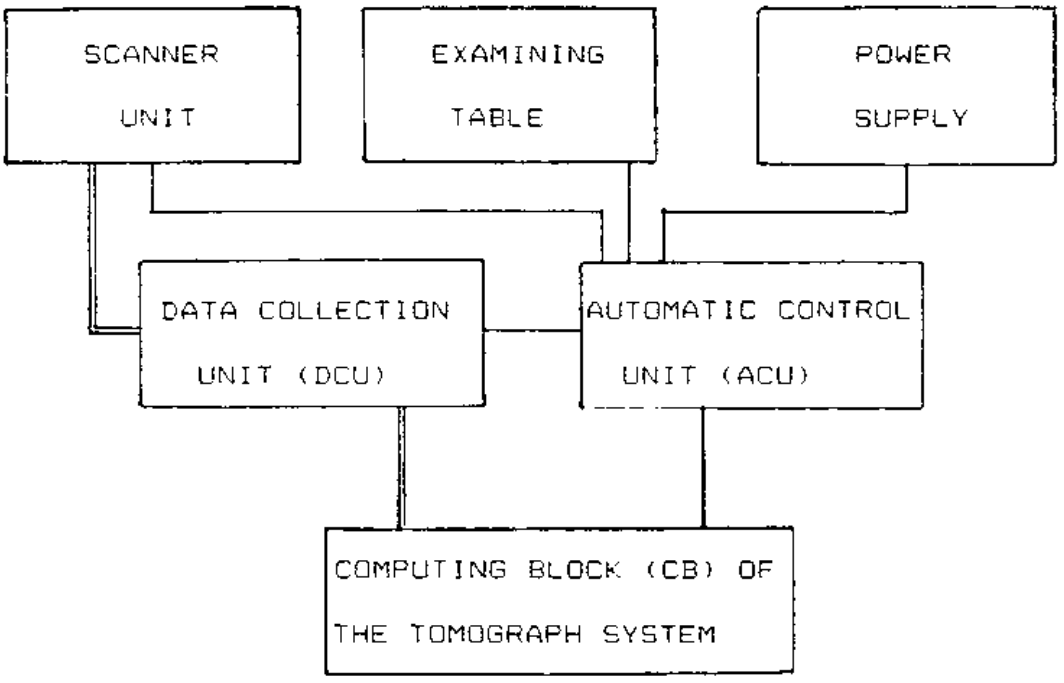

Fig. 1. Position of the computing block in the tomography system

The computing block of the CXTU is unique by virtue of a number of functional blocks that are now being designed for it (Fig. 2). A personal computer is used as the control unit for the CB. The bulk of the computations is handled by a special processor. The operator interface is effected through a keyboard, a mouse, and a special control console. A video display and a hard-copy output are provided.

Image data from the DCU are passed into the special processor where the basic computational tasks of image restoration are performed: the preliminary processing (PP) of raw data, the projection filtering (PF), and the reverse projection (RP).

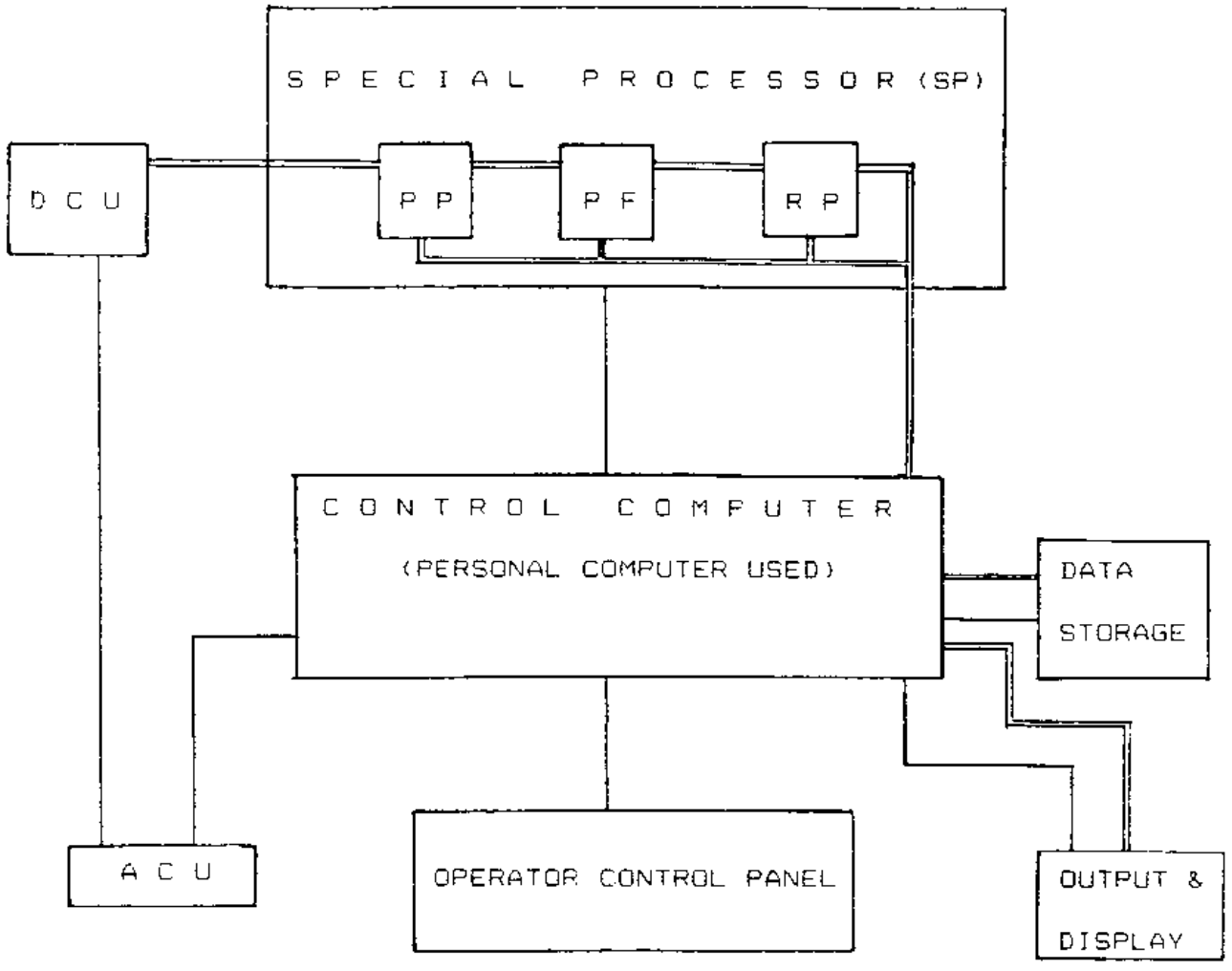

Fig.2. Functional block diagram of the CB

The matrix of the reconstructed image is filtered in the special processor in accordance with a given algorithm and passed on to the control computer. Data from the DCU and the reconstructed images are recorded on magnetic disks or tape. Data compression techniques may be used in the process.

The PP block performs the verification and error correction of sensor data, subtracts the "substitution value", converts the results obtained into a logarithmic form, corrects for radiation dispersion, normalizes the channels to compensate for their nonuniformity, receives the outputs from the support sensors, and corrects for the polychromaticity of the X-ray emission. All these functions are not computation-intensive and are executed in the PP block at the rate at which the projections are introduced.

The projection filtering utilizes various functions (nuclei): those of Shepp-Logan, Lakshminarayan-Ramachandran, Reece, Tuci and others. The PF block processes the projections at the rate at which they arrive from the PP block.

Particular complications in the design of the CB arise from the special-processor block, which implements the reverse-projection algorithm and which must process the data at a high speed. The reverse-projection algorithm can be readily made to work in a parallel fashion, which simplifies the task of designing a high-speed RP block, and may be accomplished by various means, for example:

1. The image matrix is broken up into quadrants or strips. Each portion of the matrix is reconstructed by a separate processing block (PB). Complete filtered projections are fed to the input of each PB, and each PB outputs its portion of the reconstructed image (Fig. 3).

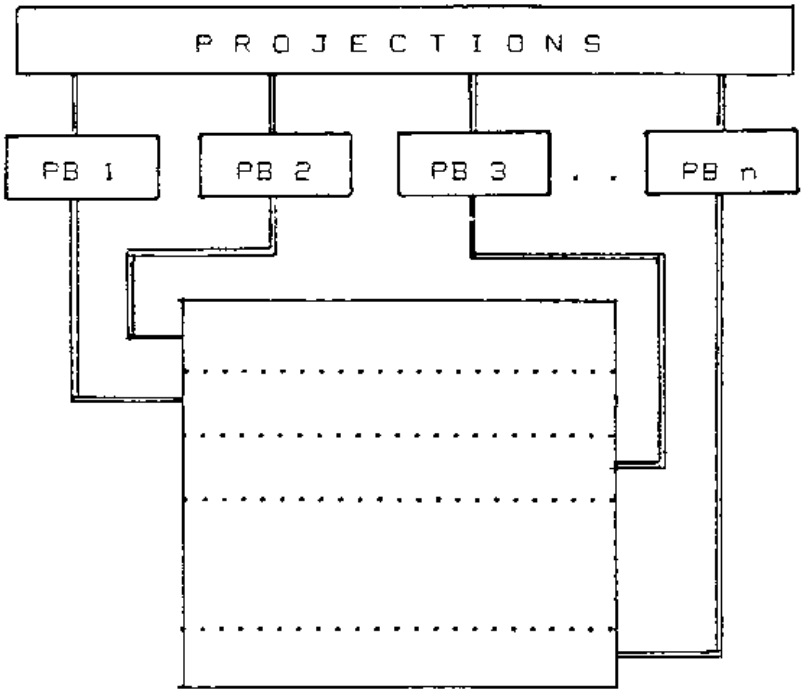

Fig.3 Parallel operation of the RP block (version 1).

2. The RP block contains several PBs each of which computes a value to be added to an element of the matrix that is being reconstructed on the basis of a given filtered projection. Connected in series, the PBs constitute a conveyor in which the summary addition to the matrix elements is accumulated for all the projections that are being processed simultaneously (Fig. 4).

In each version, the number of the PBs selected is based on their efficacy and on the time required for the generation of a tomogram after the scanning has been completed. If the cumulative

speed of processing of the projections in the RP block is lower than the rate at which the projections arrive from the PF block, a RAM buffer is used to compensate for the difference in speed.

In order to test the separate blocks of the special processor and to evaluate the repetitive image reconstruction, a feature is being implemented which will permit loading the initial data into the special processor from the control computer (CC), and unloading the results into the CC, after processing the data by the PP and PF blocks.

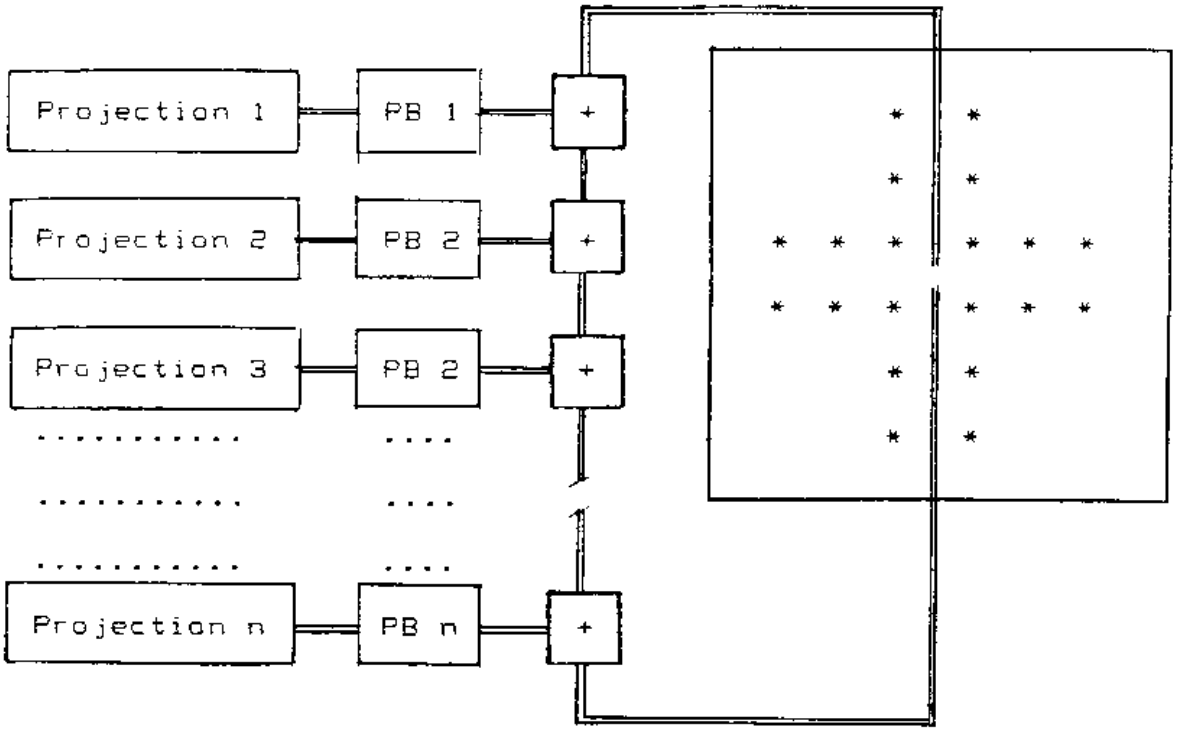

Fig.4. Parallel operation of the RP block (version 2).

The special processor may be implemented as a hardware algorithm for image reconstruction or as a universal multi-processing computational accelerator.

Software

The tomograph software (TS) must offer the operator maximal convenience in both the examination of the patient and in processing of the resultant data.

To this end, subsystems are being developed that will provide the following features:

-A library of readily selectable, standard routines for the examination of the head, neck, chest, abdomen, and the extremities.

- A means of registering a new patient and accessing a catalog of patients who had been examined in the past.

-A means of "bench marking" the patient with reference to the examining table and generating tomographic sections by using topograms to aim at targets.

-A means of visualizing and analyzing of tomograms.

-Repetitive image reconstruction in areas of interest based on prior projection data.

-Generation of sagittal and coronary sections.

-Construction of three-dimensional images based on multiple sections.

-Preparation of documentation with hard-copy capability.

-Operational aids for the operator such as a menu and a brief listing of capabilities available at any given point in the examination process.

The software provided for the visualization and analysis of the tomograms enables the operator to select the most convenient graphical technique, e.g.:

-A dot cursor for designating a point on the tomogram.

-A line cursor to indicate a vertical or horizontal line on the tomogram.

-A "frame" in the shape of a rectangle, circle, ellipse or any arbitrary enclosed curve to define the area of interest.

-Segments of angles and grids for geometric measurements.

-An arrow to mark and select various areas on the monitor screen.

The following capabilities are available in the tomogram analysis mode:

-Determination of density at a given point.

-Availability of statistical data for the area of interest (average density, minimum and maximum density values, dispersion, and standard deviation).

-Generation of a density distribution plot along a line cursor.

-Generation of a density distribution histogram for a designated area of interest.

-Measurement of distances and angles constructed by segments.

-Measurement of the area of interest.

-Use of various filters for image processing (smoothing, contrast-enhancement).

-Magnification of a selected portion of the image by 2X to 10X.

-Rotation of the image through 90, 180, and 270 degrees.

-Symmetrical transformation with respect to the vertical or horizontal axes.

-Generation of negative images.

-Subtraction and addition of images.

-Adjusting of boundaries of the visible density interval.

-Adjusting of the density transformation function in grey levels when in tomogram visualization mode.

When in documentation mode, the TS will have the capability to superimpose comments onto the image, assemble anywhere from two to nine images into one document, and provide a hard-copy output.

Currently in design are subroutines which will provide the following capabilities:

-Adjustment of the individual subsystems of the tomograph.

-Calibration of the data collection system.

-Adjustment of sensors.

-Testing.

All the subsystems are controlled by one unit. To this end, an appropriate programming shell is being developed.

Status of the project, current problems.

The computing block and the software portion of the tomograph project are in the development stage. The overall architecture of the computing block has been defined. The communication hardware for linking the tomograph subsystems is being built for the laboratory prototype unit. The special processor is being designed and built in two versions: as a universal processor and as a processor in which the image reconstruction algorithm is implemented in hardware. The development of software for the visualization and image analysis functions is 50% complete. The software for the control of the tomograph subsystems is in design.

The problem is the absence of high-speed LSI chips suitable for the creation of a compact and reliable special processor.